

 Open access • Proceedings Article • DOI:10.1109/ICSMC.2003.1245665

A simulation of attempts to influence crowd dynamics — [Source link](#)

J.A. Kirkland, Anthony A. Maciejewski

Institutions: Colorado State University

Published on: 17 Nov 2003 - Systems, Man and Cybernetics

Topics: Social force model and Crowds

Related papers:

- [Social Force Model for Pedestrian Dynamics](#)
- [Simulating dynamical features of escape panic](#)
- [Experiments in Automatic Flock Control](#)
- [A Fluid-Dynamic Model for the Movement of Pedestrians](#)
- [A Cellular automaton model for crowd movement and egress simulation](#)

Share this paper:    

View more about this paper here: <https://typeset.io/papers/a-simulation-of-attempts-to-influence-crowd-dynamics-2m5mo7spdg>

A Simulation of Attempts to Influence Crowd Dynamics¹

Joel A. Kirkland Anthony A. Maciejewski
Department of Electrical and Computer Engineering
Colorado State University
Ft. Collins, CO 80523-1373 USA
jkirklan@lamar.colostate.edu
aam@colostate.edu

Abstract – *An understanding of how to alter crowd dynamics would have a significant impact in a number of scenarios, e.g., during riots or evacuations. The social force model, where individuals are self-driven particles interacting through social and physical forces, is one approach that has been used to describe crowd dynamics. This work uses the framework of the social force model to study the effects of introducing autonomous robots into crowds. Two simple pedestrian flow problems are used as illustrative examples, namely flow in varying width hallways and lane formation in bidirectional pedestrian flow. Preliminary results indicate that robots capable of inducing an attractive social force are effective at improving pedestrian flow in both of these scenarios.*

Keywords: crowd dynamics, pedestrian lane formation, agent-based modeling

1 Introduction

The study of crowd dynamics, or the large-scale motion of people, has an impact on a wide range of applications including architecture, pedestrian transportation, escape planning, stampedes, event organization, and crowd control. Architects and transportation designers frequently use crowd dynamics in the design of outdoor and indoor environments to increase the ease and efficiency of everyday pedestrian flow. Furthermore, under more extreme conditions such as stampedes and fire escapes, improved procedures and building layouts could save lives. Recently in the Chicago Stampede, the use of pepper spray to break up a fight in a nightclub caused the crowd to surge down a stairwell killing or injuring over 70 people [2]. Additionally, in a Rhode Island nightclub, a fire, started by a pyrotechnic display, rapidly spread and overtook the crowd attempting to escape through the clogged front exit killing 97 people [3]. Both disasters occurred in February of 2003 and demonstrate the immediate need for directing large groups of people in emergencies.

Previous work to quantify pedestrian flows and crowd dynamics has been studied primarily through simulating the motion of individuals. For example, Blue [1] used a cellular automata model to generate emergent lane formation. Though not for groups of people, Reynolds [8] used an agent-based model to generate flocking behavior using a small set of simple interacting rules for each agent. Along a similar line, Helbing, Molnar, and Vicsek [6] have used a social force model to demonstrate lane formation and the physical jamming at bottlenecks during panics and stampedes.

We have used the social force model as a foundation for our simulations of pedestrian flow and crowds. We have augmented the model with the addition of dissimilar agents, i.e., autonomous robots. These additional agents are used to perform various maneuvers and to interact under different rules. Our ultimate goal is to increase large-scale organizational patterns such as lane formation, and to reduce disorganization such as jamming at bottlenecks.

2 Social Force Model

The social force model was first introduced by Helbing and Molnár [5] and has been expanded to include physical contact forces (with similarities to granular flows) for panic situations [6], [7].

The social force model to describe pedestrian flow has its origins in gas-kinetic models [4]. It consists of self-driven particles, i.e., people, that interact through social rules. Each person adapts his or her current velocity to match a desired direction and a desired speed; furthermore, each crowd member simultaneously tries to avoid bumping into other crowd members and any environmental boundaries. The social interactions produce changes in the velocities and reflect a change in motivation rather than physical forces acting on the person. These social forces can be influenced by the environment, other people, and internal states.

¹ This work was supported by the Non-lethal Technology Innovation Center, University of New Hampshire.
0-7803-7952-7/03/\$17.00 © 2003 IEEE.

2.1 Basic Social Force Equations

For a crowd consisting of N individuals, the force acting on the i th person is denoted by f_i and is given by

$$f_i = f_i^S + \sum_{\substack{j=1 \\ i \neq j}}^N f_{ij}^I + \sum_{k=1}^M f_{ik}^W \quad (1)$$

where f_i^S denotes the self-driven force that drives an individual towards their desired velocity, f_{ij}^I denotes the interaction force on individual i due to individual j , and f_{ik}^W denotes the wall avoidance force due to the k th wall (out of a total of M wall surfaces). The self-driven force is based on a simple error correction term consisting of the difference between an individual's desired velocity, denoted by a desired speed s_i and a desired direction \hat{e}_i , and their actual velocity denoted by v_i . This difference in velocity is corrected over a specified time interval τ_i , which is referred to as the relaxation time, that corresponds to the finite amount of time that is required for people to react and physically change their velocity. Thus the self-driven force is given by

$$f_i^S = \frac{m_i(s_i \hat{e}_i - v_i)}{\tau_i} \quad (2)$$

where m_i denotes the mass of the i th individual.

The person-to-person interaction force consists of two major components, i.e., a social interaction term and a physical interaction term. The social interaction term is used to represent an individual's inherent desire to maintain a certain amount of personal space. It is modeled as a repulsive force from other individuals that decreases with distance. The distance between individuals i and j is given by

$$d_{ij} = \|\mathbf{x}_i - \mathbf{x}_j\| - r_i - r_j \quad (3)$$

where \mathbf{x} is the position of an individual and r is their radius, i.e., people are modeled as circles. The exponential function is used to represent the manner in which the social interaction force decreases, with the magnitude (strength) of the interaction given by the parameter A and the distance over which it is active given by the parameter B , so that the entire expression for this term is given by $A \exp(-d_{ij}/B)$.

In some cases, such as in panic or high-density situations, physical contact between individuals occurs and can become a significant factor. The physical interactions consist of a body compression term and a tangential friction term. The compressional term acts along the unit vector, $\hat{\mathbf{n}}_{ij}$, given by

$$\hat{\mathbf{n}}_{ij} = (\mathbf{x}_i - \mathbf{x}_j) / \|\mathbf{x}_i - \mathbf{x}_j\| \quad (4)$$

with a magnitude given by the parameter k . The frictional component acts along the tangential unit vector

$\hat{\mathbf{t}}_{ij}$, which is orthogonal to $\hat{\mathbf{n}}_{ij}$, and is proportional to the difference in tangential velocity given by

$$\Delta v_{ij}^t = (\mathbf{v}_i - \mathbf{v}_j) \cdot \hat{\mathbf{t}}_{ij} \quad (5)$$

The magnitude of this sliding frictional term can be set using the parameter κ . Combining the social and physical forces together yields:

$$f_{ij}^I = \left[A^I \exp(-d_{ij}/B^I) + k^I g(d_{ij}) \right] \hat{\mathbf{n}}_{ij} - \left[\kappa^I g(d_{ij}) \Delta v_{ij}^t \right] \hat{\mathbf{t}}_{ij} \quad (6)$$

where the function $g(x)$ is zero if x is positive and returns $-x$ if x is negative so that there is no contribution from the physical forces when people are not in contact.

The equation for interactions between a person and a wall is analogous to the social interactions between people and is given by:

$$f_{ik}^W = \left[A^W \exp(-d_{ik}/B^W) + k^W g(d_{ik}) \right] \hat{\mathbf{n}}_{ik} - \left[\kappa^W g(d_{ik}) v_i \cdot \hat{\mathbf{t}}_{ik} \right] \hat{\mathbf{t}}_{ik} \quad (7)$$

where d_{ik} is now the minimum distance separating individual i from the k th wall, $\hat{\mathbf{n}}_{ik}$ is the unit vector along this minimum distance, and $\hat{\mathbf{t}}_{ik}$ is perpendicular to $\hat{\mathbf{n}}_{ik}$.

2.2 Introducing a Heterogeneous Mixture

The previous section presented an overview of the social force model used by Helbing [4-7] to describe the behavior of people in crowds. Our goal is to determine if one can modify the dynamics of a crowd in a desired manner by introducing autonomous robots to obtain a heterogeneous mixture of agents. The behavior of the robots are modeled using the same basic social force model given in (1), however, they can attempt to influence behavior through a desired velocity that is different from the people in the environment. In addition, the interaction parameters A^I and B^I can be altered, and in fact, there will now exist four different versions of these parameters corresponding to the four scenarios:

1. Person responding to another person
2. Person responding to a robot
3. Robot responding to a person
4. Robot responding to another robot

Although there is little experimental data for determining the parameter values for scenario 2, the interaction parameters for scenarios 3 and 4 can be set over a wide range since these represent the programming of the robot's behavior.

We have also introduced an additional cohesive social force interaction term to (6) that is meant to model the affect of a robot on a person when the robot is using some visual or auditory cues to direct the motion of individuals in the crowd toward the robot. This force term is given by $C \exp(-[d_{il} - D]^2/E) \hat{\mathbf{n}}_{il}$ where C is the magnitude of the attraction force, D is the distance

where the attraction force is greatest, and E represents how quickly the force decreases with distance. The robots are programmed to respond with an identical cohesive force, i.e., they are attracted towards people.

3 Simulations

Our initial simulations considered two simple pedestrian flow scenarios previously studied by Helbing, namely unidirectional pedestrian flow through a hallway that contains a widening and bi-directional pedestrian lane formation in a corridor. The parameters used in the simulations were similar to those used in [6] and are given in Table 1. For simplicity, all of the interaction parameters are identical for each person and each robot. In addition, the person/agent parameters are identical, except that the radius of people is randomly selected from a uniform distribution between 0.25-0.35 m with robots all being 0.35 m in radius.

Interaction		Person/Agent	
A	2000 N	m	80kg
B	0.08 m	s	1.2 or 3 m/s
C	-600 to 0 N	τ	0.5 s
D	0.5 m	r	0.25 to 0.35 m
E	0.05 m ²		
k	1.2 x 10 ⁵ kg/s ²		
κ	2.4 x 10 ⁵ kg/ms		

A standard measure of pedestrian flow efficiency is used to measure the impact of introducing robots into the environment. Efficiency is defined as the ratio of the average speed of the individuals in their desired direction to their desired speed in that direction, i.e.,

$$\text{EFFICIENCY} = \frac{\left(\sum_{i=1}^n \hat{e}_i \cdot v_i / n \right)}{s} \quad (8)$$

where n is the number of pedestrians within the region of interest over which the efficiency is calculated. (For our simulations all individuals have the same desired speed.) This measure is typically between 0 and 1, however, negative values are possible (if the average velocity is in a direction opposite of that desired) as well as values greater than 1 (if external forces propel individuals in their desired directions). For each simulation run, the initial location of pedestrians is randomly determined and a sufficient number of trials are executed in order to obtain a 95% confidence interval for the mean efficiency.

In all simulation displays, green (lighter) circles indicate people traveling to the right, the blue (darker) circles indicate people traveling to the left, and the red squares indicate robots. The internal arrows indicate the

desired direction of travel \hat{e}_i ; rather than the actual velocity or resultant forces.

3.1 Hallway with a Widening

Our first set of simulations consisted of pedestrian flow through a hallway with a widening without any robots (see Fig. 1). The hallway was 3 m wide and the widening was 6 m long and 9 m at the widest point. Each robot and pedestrian's desired speed was set at a relatively high 3 m/s. After a pedestrian passes through the widening they are removed and replaced by a new pedestrian at a random starting location, i.e., at the extreme left of the hallway, to maintain a constant number of people in the hallway. The mean efficiencies (measured in the widened area) for 40, 50, and 60 people were 0.82 ± 0.04 , 0.73 ± 0.01 , and 0.67 ± 0.02 , respectively. These results are consistent with those obtained by Helbing [6], who also found reduced efficiency due to the tendency for pedestrians to take advantage of the widened area to increase their personal space and then create bottlenecks and clogging when the hallway is again restricted.

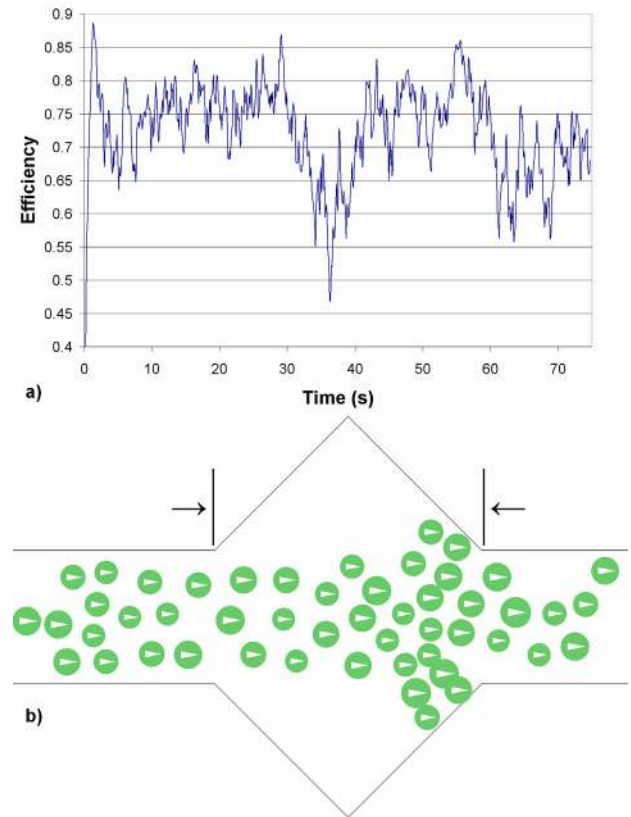


Figure 1: Typical simulation results for pedestrian flow through a hallway with a widening. Part (a) shows a plot of the instantaneous efficiency within the widened area of the hallway (between the two arrows). Part (b) shows a snapshot of the simulation at 36 s, which has a particularly low efficiency. Note the arching of the flow at the end of the widening which causes the inefficient flow. This run had 50 people.

3.1.1 Maneuvers and Formations

Our initial attempts to reduce the disturbances caused by the widening of the hallway consisted of introducing additional agents that performed various maneuvers to encourage the pedestrian flow to remain contained throughout the widening. Two types of maneuvers were simulated, namely a set of 2-6 robots moving in a triangular pattern within the triangular shape of the widening (counter-clockwise on top, clockwise on the bottom) and two robots traveling back and forth across the widening.

The resulting efficiencies for these various scenarios are presented in Fig. 2. There is not a statistically significant difference in the mean efficiencies resulting from the type of maneuver executed or the number of robots used in the maneuver. The main finding of these experiments is that robots can be effective for increasing efficiencies at low pedestrian densities; however, their efficacy diminishes as the pedestrian density increases.

Fig. 3 presents an example of a case where the triangular maneuver is successful at preventing the pedestrian flow from extending into the widened area and thus increasing efficiency. However, as pedestrian densities increase, the potential increases for large groups of people to create significant physical and social repulsion forces that make the robots deviate from their desired trajectory. An extreme example of this is illustrated in Fig. 4, where a robot is swept away from its intended maneuver. Clearly, forcing the robots to be stationary can prevent this from occurring. In fact, our results show that properly positioned stationary robots can produce efficiencies that are comparable to an equal number of robots performing the back-and-forth maneuvers.

3.1.2 Cohesive Social Forces

Our second set of attempts to reduce the disturbances caused by the widening of the hallway involved having the robots within the flow of pedestrians rather than maneuvering strictly in the widened area. Thus, as with the pedestrians, this requires that robots be removed from the right side of the hallway and replaced at the left. We assume that these robots are equipped with mechanisms that create the mutual social attraction forces discussed in section 2.2, e.g., the ability to identify people and deliver verbal or visual instructions.

Fig. 5 shows the efficiencies resulting from introducing robots with a social attractive force into the hallway. This force is effective in improving pedestrian flow by reducing the number of individuals spreading into the widened area and thus reducing the disturbances that occur when the widening is restricted. An example of this is shown in Fig. 6.

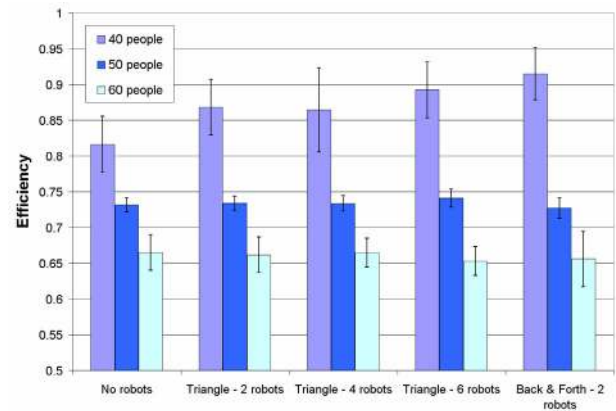


Figure 2: Resulting mean efficiencies for two different types of maneuvers by different numbers of robots and different pedestrian densities. In general, robot maneuvers tend to increase efficiencies at low pedestrian densities but have little or no effect at high pedestrian densities.

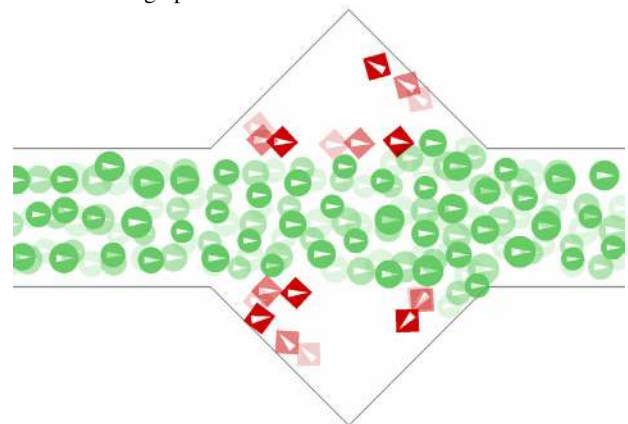


Figure 3: An example of robots executing a triangular pattern maneuver that is successful in increasing pedestrian efficiency. Three consecutive snapshots taken 0.25 s apart are shown overlapped to illustrate the motion (the darker the figure the more recent the snapshot). This simulation included 50 pedestrians and resulted in a mean efficiency of 0.76 over this 1 s interval.

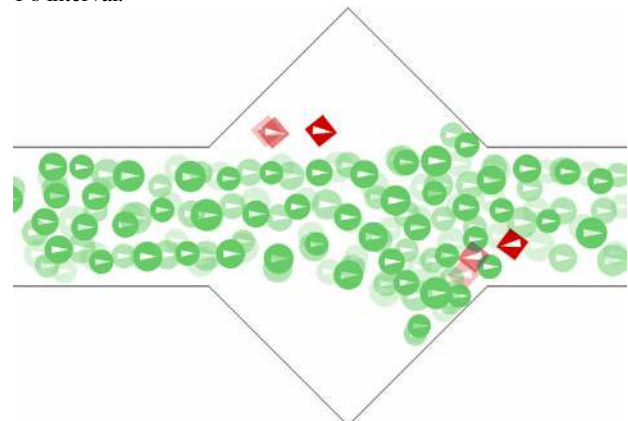


Figure 4: An example of robots executing a back-and-forth pattern maneuver illustrating the risk of robots being swept away from their desired trajectories due to being overwhelmed by the physical and social repulsion forces. Three consecutive snapshots taken 0.5 s apart are shown overlapped to illustrate the motion (the darker the figure the more recent the snapshot). This simulation included 50 pedestrians.

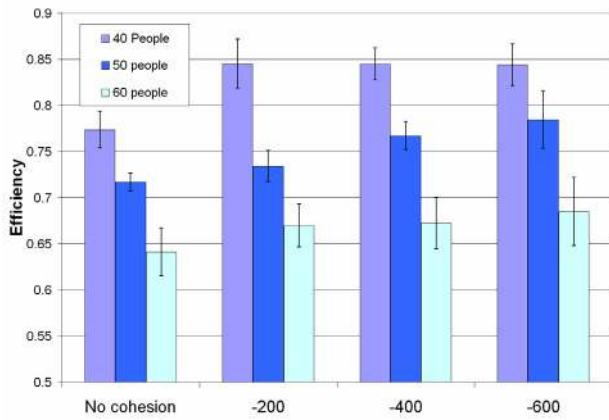


Figure 5: Resulting mean efficiencies as a function of the magnitude of the social attraction force and different pedestrian densities. In general, efficiency is increased by the introduction of an appropriate social attraction force

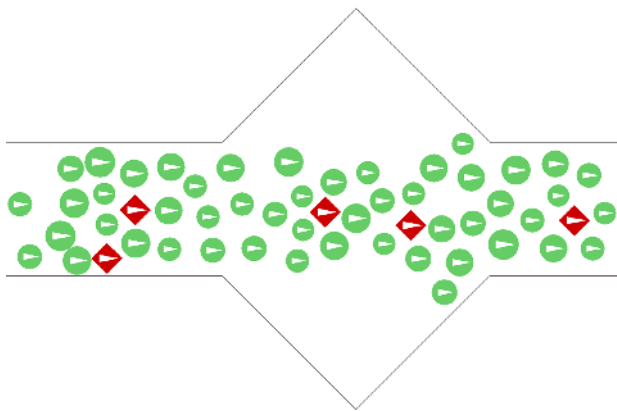


Figure 6: An example of increased efficiency due to the introduction of robots with a social attraction force. These forces prevent the flow of pedestrians from expanding into the widened area of the hallway. The magnitude of the attractive force was given by $C = -400$ N. This simulation run included 50 people, five robots, and resulted in a mean efficiency of 0.78.

3.2 Lane Formation

Our second set of simulations was centered on the lane formation phenomenon that occurs as an emergent property of the many interactions within bidirectional pedestrian flows. These lanes vary dynamically in number, size, and longevity. An example of lane formation is presented in Fig. 7, which shows the results of a simulation for a 7 m wide and 30 m long hallway that contained 140 pedestrians with half moving in each direction at a desired speed of 1.2 m/s. (Previous work [5] has shown that at this width the average expected number of lanes is three.) While directly measuring the presence of lanes is somewhat ill defined, it has been shown that efficiency is highly correlated to well-formed lanes (see Fig. 7) so that we use efficiency as our measure of lane formation. The mean efficiency, calculated over the entire population, was 0.60 ± 0.02 .

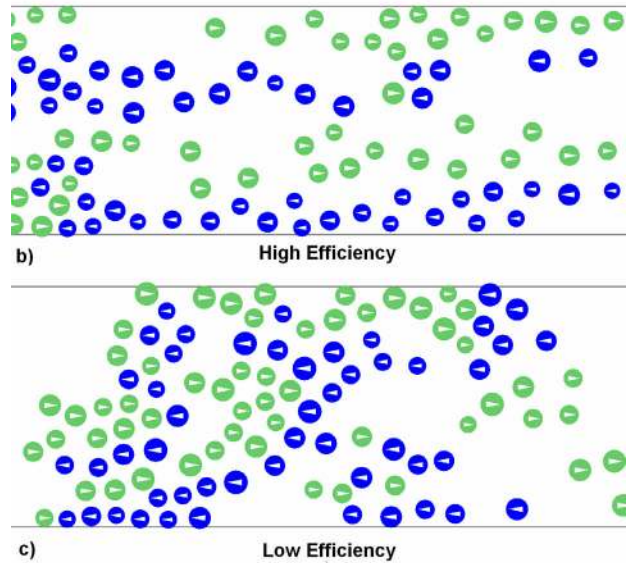
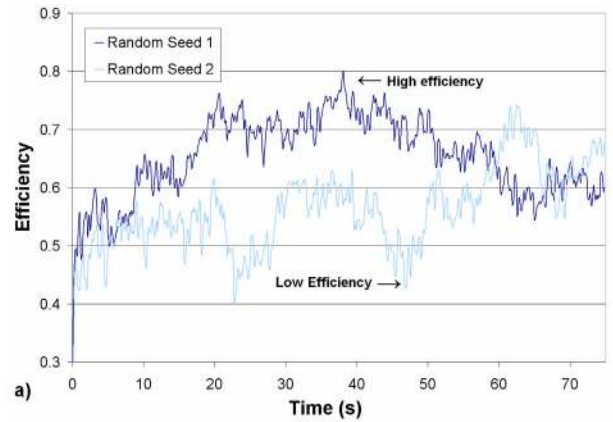


Figure 7: Typical simulation results for lane formation in bidirectional pedestrian flow through a hallway. Part (a) shows a plot of the instantaneous efficiency. Part (b) shows a snapshot of the simulation at 38 s, which has a particularly high efficiency of 0.80. Note the four very well formed lanes. Part (c) shows a snapshot of the simulation at 47 s, which has a particularly low efficiency of 0.44. Note the clumping of pedestrians traveling in opposing directions. The average efficiency for the two runs was 0.67 and 0.57.

3.2.1 Maneuvers and Formations

Our first attempts to encourage lane formation involved introducing robots moving in rectangular and figure eight patterns to encourage two and three lanes respectively; however, we found that any crossing of the pedestrian flows produced significant disturbances to any lanes, resulting in much lower efficiencies than compared to efficiencies without additional agents.

Our next attempt to encourage lane formation was to introduce stationary patterns that shift the pedestrians into two or three lanes. Two such patterns are illustrated in Fig. 8, i.e., the 1×5 pattern consisting of a single diagonal set of five robots to induce two lanes and the funnel pattern used to induce three lanes. The 1×5 pattern was one of the best patterns tested and resulted

in a statistically significant improvement over the nominal efficiency (0.69 ± 0.03 compared to 0.60 ± 0.02). The funnel pattern, which was the only pattern tested that attempted to induce three lanes, did not result in any improvement in efficiency over the nominal case.

3.2.2 Cohesive Social Forces

Our final set of attempts to induce lane formation involved the introduction of robots capable of creating the social attraction forces discussed in section 2.2. Eight such robots were included in the hallway with four traveling in each direction. As the robots reached the end of the hallway, they were restarted at the same initial location at the opposite end of the hallway. The introduction of these robots was successful at increasing the amount of lane formation as measured by the efficiency. In particular, the efficiency obtained by using an attraction force magnitude of -800 N was 0.67 ± 0.03 . An example from one simulation run is presented in Fig. 9.

4 Conclusions

The results presented here are very preliminary and do not address many of possible variations in parameters and strategies for influencing crowd dynamics. However, several conclusions can be drawn even from the initial results presented here. First, the dynamics of crowd behavior are highly complex and are not well understood. The introduction of autonomous robots into such an environment can alter the dynamics to produce some desired behaviors. In particular, we have shown that robots that can implement an attractive social force can be effective at improving pedestrian flow in different scenarios. However, great care must be taken when introducing robots into such environments because it is not uncommon for apparently reasonable robot behaviors to have unexpected deleterious effects.

References

[1] V. J. Blue, "Cellular automata microsimulation for modeling bi-directional pedestrian walkways," *Transportation Research, Part B: Methodological*, Vol. 35, No. 3, pp. 293-312, Mar. 2001.

[2] CNN.com, "Official: Chicago club was told to close second floor," Feb. 19, 2003, <http://www.cnn.com/2003/US/Midwest/02/17/chicago.nightclub/index.html>

[3] CNN.com, "At least 96 killed in nightclub inferno," Feb. 21, 2003, <http://www.cnn.com/2003/US/Northeast/02/21/deadly.nightclub.fire/index.html>

[4] D. Helbing, "A fluid dynamic model for the movement of pedestrians," *Complex Systems*, Vol. 6, No. 5, pp. 391-415, 1992.

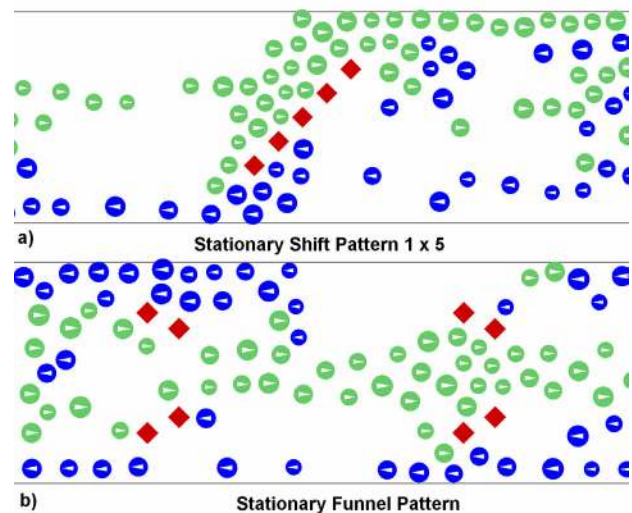


Figure 8: Examples of attempting to induce lane formation by using stationary robots in particular patterns. Part (a) shows the 1×5 pattern designed to form pedestrians into two lanes while part (b) shows the funnel pattern that was designed to form three lanes. The mean efficiencies for the 1×5 pattern and the funnel pattern are 0.69 ± 0.03 and 0.59 ± 0.02 , respectively.

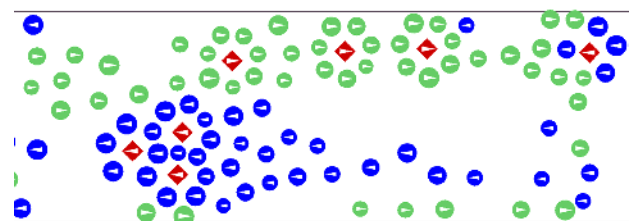


Figure 9: An example of increased efficiency due to the introduction of robots with a social attraction force. These robots have been successful in forming two well formed lanes. The simulation included 140 people and eight robots. The magnitude of the attractive force was given by $C = -800$ N.

[5] D. Helbing and P. Molnar, "Social force model for pedestrian dynamics," *Physical Review E*, Vol. 51, No. 5, pp. 4282-4286, May 1995.

[6] D. Helbing, I. Farkas, and T. Vicsek, "Simulating dynamical features of escape panic," *Nature*, Vol. 407, pp. 487-490, Sep. 28, 2000.

[7] D. Helbing, "Traffic and related self-driven many-particle systems," *Reviews of Modern Physics*, Vol. 73, No. 4, pp. 1067-1141, Oct. 2001.

[8] C. W. Reynolds, "Flocks, herds, and schools: A distributed behavioral model," *Computer Graphics*, Vol. 21, No. 4, pp. 25-34, 1987.